

REPORT



## Native peptide mapping – A simple method to routinely monitor higher order structure changes and relation to functional activity

Michel Degueldre <sup>a</sup>, Annemie Wielant<sup>a</sup>, Eglantine Giroto<sup>a</sup>, Will Burkitt<sup>b</sup>, John O'Hara<sup>b</sup>, Gaël Debaue <sup>a</sup>, Annick Gervais<sup>a</sup>, and Carl Jone<sup>a</sup>

<sup>a</sup>Department of Analytical Science Biologicals, UCB, Braine L'Alleud, Belgium; <sup>b</sup>Department of Analytical Science Biologicals, UCB, Slough, UK

### ABSTRACT

In the biopharmaceutical environment, controlling the Critical Quality Attributes (CQA) of a product is essential to prevent changes that affect its safety or efficacy. Physico-chemical techniques and bioassays are used to screen and monitor these CQAs. The higher order structure (HOS) is a CQA that is typically studied using techniques that are not commonly considered amenable to quality control laboratories. Here, we propose a peptide mapping-based method, named native peptide mapping, which could be considered as straightforward for HOS analysis and applicable for IgG4 and IgG1 antibodies. The method was demonstrated to be fit-for-purpose as a stability-indicating assay by showing differences at the peptide level between stressed and unstressed material. The unfolding pathway induced by a heat stress was also studied via native peptide mapping assay. Furthermore, we demonstrated the structure–activity relationship between HOS and biological activity by analyzing different types of stressed samples with a cell-based assay and the native peptide mapping. The correlation between both sets of results was highlighted by monitoring peptides located in the complementary-determining regions and the relative potency of the biotherapeutic product. This relationship represents a useful approach to interrogate the criticality of HOS as a CQA of a drug.

### ARTICLE HISTORY

Received 21 January 2019  
Revised 11 June 2019  
Accepted 18 June 2019

### KEYWORDS

Higher Order Structure; monoclonal antibody; peptide mapping; Method Development; mass spectrometry; quality control; structure activity relationship; Bioassay; Biopharmaceutical; stability

## Introduction

Regulatory agencies and the pharmaceutical industry increasingly expect that the entire manufacturing process will be driven by good manufacturing practices (GMP).<sup>1–3</sup> Therefore, the process of defining and controlling product critical quality attributes (CQA), which are defined by the quality by design approach (QbD),<sup>4–6</sup> is crucial, and ensures that the safety and efficacy of the product are maintained.<sup>7</sup> The higher order structure (HOS) of a product, which may be considered a CQA, can be studied by a wide range of techniques, such as fluorescence detection,<sup>8</sup> circular dichroism,<sup>9–13</sup> X-ray crystallography,<sup>14–16</sup> nuclear magnetic resonance (NMR),<sup>17–19</sup> epitope detection and Fourier-transform infrared spectroscopy.<sup>20–23</sup> This characterization approach is in line with the U.S. Food and Drug Administration's Quality by design (QbD) initiative<sup>24</sup> linking a desired product quality with physico-chemical or biological properties/characteristics.<sup>25</sup> Information gathered during this testing is of great value in terms of product knowledge, providing a link between result values and the corresponding CQAs, but it is also valuable for product developability assessment.<sup>26</sup> The knowledge gained from this developability assessment can be used to guide the process and product development to reduce timelines and resource consumption.

Mass spectrometry (MS) has become the gold standard as a tool to characterize biologic protein products. This was demonstrated by Rogstad *et al.* based on the number of submitted biologics license applications in which MS was extensively used within the characterization section.<sup>27</sup> In addition, Rathore *et al.*

showed the capability of emerging MS-based applications in product development, such as comparability, biosimilarity, and quality control.<sup>28</sup> For instance, an advance in HOS analysis and the relation between drug structure and activity for a therapeutic monoclonal antibody (mAb) using hydrogen/deuterium exchange MS was reported in 2016 by Yan *et al.*<sup>29</sup> In this work, the authors highlighted that oxidation and aspartic acid isomerization, which are included in complementary-determining region 2 (CDR2) of a mAb heavy chain, modify the binding of the mAb with its respective antigen in an enzyme-linked immunosorbent assay (ELISA). Another MS-based method was developed by Gau *et al.*<sup>30</sup> based on the fast photochemical oxidation of proteins. In this technique, the reaction between a radical and a residue side chain is used to evaluate the solvent accessibility of the residue, which is determined by the protein's tertiary and quaternary structure. The identification of the protein's oxidized residues gives information on the HOS of the protein.

Using high-resolution 2D NMR, a recent interlaboratory study demonstrated the precision and robustness of the technique for HOS comparison of four different filgrastim molecules (1 innovator product compared to 3 biosimilar products). The study allowed differentiation between different products.<sup>19</sup>

A significant disadvantage of existing HOS analysis techniques is their lack of applicability within a routine quality control (QC) environment. The techniques require expensive equipment, highly trained operators, complex post-acquisition treatment of data and software that would comply with the data integrity requirements prescribed in cGMP.<sup>31</sup> In addition to these

requirements, it is difficult to set simple acceptance criteria to control HOS for these state-of-the-art techniques.

Perrin *et al.*<sup>32</sup> recently reported a method to perform limited proteolysis<sup>33–35</sup> of mAbs in native-like conditions. In this approach, the protease cleaves the protein backbone in locations that are accessible to the protease. The authors followed Lys-C enzymatic digestion kinetics via liquid chromatography hyphenated to tandem MS (LC-MS/MS), and observed significant differences between native mAb and deglycosylated mAb in terms of the rates of peptides released by the Lys-C digestion. Their results demonstrated the suitability of limited proteolysis and LC-MS/MS for the analysis of HOS in a biopharmaceutical environment.<sup>32</sup> More recently, Cao *et al.* applied a limited proteolysis method to different stressed samples with MS equipment easily amenable to a QC environment. This and other limited proteolysis methods have been used to discriminate stressed and unstressed material.<sup>32,36</sup>

Here, we have further developed the method so that, in addition to its routine use to support process, formulation development and stability studies, the method yields predictive information on the biological activity of the drug. The initial work was conducted to identify all the peptides that are cleaved by the trypsin in native-like conditions by matrix-assisted laser desorption ionization mass spectrometry (MALDI) coupled with high-resolution mass spectrometry. Because the biopharmaceutical industry pipeline includes different subtypes of mAbs, we applied our method to two of the most common subtypes: IgG4 and IgG1 antibodies. To demonstrate the high capacity of the method to extract information on the biotherapeutics structure during stress conditions, we followed the unfolding pathway of the IgG4 molecule by the native peptide mapping during heat stress. In parallel to the unfolding pathway study by native peptide mapping, the unstressed and stressed materials were analyzed by a cell-based assay (CBA) in order to give information on the activity of the drug. A correlation was shown by comparing the structural integrity of the mAb (HOS information given by the native peptide mapping) and its activity by the bioassay. Finally, the same strategy was applied to multiple-stressed samples to clearly demonstrate the relationship between the native peptide mapping and the bioassay. These studies were useful in defining what changes to the HOS of the mAb were critical to maintain the biological activity of the molecule.

## Results

### **Development of the native peptide mapping method and its extension in a QC routine environment**

The IgG4 mAb samples were subjected to limited proteolysis in native-like conditions for a range of time periods. To maintain the native conditions of the sample, it was diluted with the Hanks' Balanced Salt buffer, and proteolysis was induced by the addition of trypsin. The trypsin digestion was quenched at several time points by acidification of the sample (addition of 1% trifluoroacetic acid (TFA)). Peptides resulting from the mAb digestion were then identified using MALDI-HRMS. Table 1 summarizes the detection of the cleaved peptides with respect to the trypsin

incubation times. The number of cleaved peptides increased as a function of the trypsin incubation time. Repeatability was assessed by analyzing the same material in triplicate on two occasions. All samples had identical order of appearance of the cleaved peptides after 5-min trypsin incubation, demonstrating the repeatability of the method (see Figure 1–4 of the supplementary material).

A digestion evolution picture of the mAb during the 5 first minutes is illustrated in Figure 1 and cleaved peptides are highlighted in red. During the 5-min trypsin incubations, the first peptide from the Fc subunit was HC 390–406. Additional Fc peptides (HC 122–133 crosslinked to LC 213–219, HC 122–133 crosslinked to LC 217–219, HC 246–252, HC 286–298, HC 290–298, HC 299–314, and HC 338–357) were progressively cleaved. The first peptides identified from the Fab subunit were HC 1–19, HC 44–61, HC 77–87, LC 1–18, LC 36–47, LC 51–66, and LC 52–66 after 2 min of trypsin incubation. An (IgG1) mAb was also analyzed using the native peptide mapping method and preliminary results, which are presented and discussed in supplementary material in Table 1, demonstrate the feasibility of the method for this mAb structure.

To facilitate the native peptide mapping method applicability to a QC environment, we substituted the MALDI-HRMS instrument with an Ultra Performance Liquid Chromatography system coupled to a mass detector (UPLC-MS). This routine UPLC-MS system has already been used by Xu *et al.* and Cao *et al.* for the development of routine-driven methods for product characterization, product development and quality control of biologics.<sup>36,37</sup> The peptide list, which was made during the development stage during MALDI-HRMS analysis, was used to aid this change of instrument.

### **A molecule's unfolding pathway can be followed using native peptide mapping**

The second step in this work is the monitoring of the unfolding pathway of the molecule by the native peptide mapping in harsh temperature conditions. To evaluate whether native peptide mapping can detect changes in a mAb's HOS upon heat stress, a mAb sample was incubated at 50°C for 11 days, and stressed samples were collected on different days. Were the stress conditions to affect the HOS of the mAb, it would be expected that the profile of peptides released by the limited proteolysis would change.

After limited proteolysis for 5 min, UPLC-MS system was used to monitor cleaved peptides. Figure 2 shows the peak area of two different cleaved peptides from days 0, 1, 2, 3, 7, and 11. One peptide (in blue) HC 299–314 was detected under both stressed and non-stressed conditions. After day 1, the peak area of the cleaved peptide appeared not to increase further. In contrast, the crosslinked peptide LC 132–147-LC 196–212 (in orange) was only detected in the stressed samples and increased steadily with the duration of the stressing. Consequently, peptide LC 132–147-LC 196–212 is a marker of stress observed by UPLC-MS in this mAb under the conditions described.

In parallel, the unstressed and stressed samples were analyzed with the native peptide mapping method using MALDI-HRMS to follow the heat degradation pathway of the molecule. The results are summarized in Table 2. The sample was digested for 1 min

**Table 1.** Summary table of cleaved peptides of IgG4 mAb trypsin digestion as a function of digestion duration. Green cell: peptide is detected by MALDI-HRMS, grey cell: peptide not detected.

IgG4 mAb results						
Peptide	Trypsin digestion time (min)					
	0	1	2	3	4	5
HC 1-19	Grey	Grey	Green	Green	Green	Green
HC 39-61	Grey	Grey	Grey	Grey	Grey	Green
HC 44-61	Grey	Grey	Green	Green	Green	Green
HC 77-87	Grey	Grey	Green	Green	Green	Green
HC 122-133-LC 213-219	Grey	Grey	Grey	Grey	Green	Green
HC 122-133-LC 217-219	Grey	Grey	Green	Green	Green	Green
HC 246-252	Grey	Grey	Grey	Grey	Grey	Green
HC 286-298 G0F	Grey	Grey	Grey	Grey	Green	Green
HC 290-298 G0F	Grey	Grey	Grey	Grey	Grey	Green
HC 299-314	Grey	Grey	Green	Green	Green	Green
HC 338-357	Grey	Grey	Grey	Green	Green	Green
HC 390-406	Grey	Green	Green	Green	Green	Green
LC 1-18	Grey	Grey	Green	Green	Green	Green
LC 36-47	Grey	Grey	Green	Green	Green	Green
LC 36-50	Grey	Grey	Grey	Green	Green	Green
LC 51-66	Grey	Grey	Green	Green	Green	Green
LC 52-66	Grey	Grey	Green	Green	Green	Green

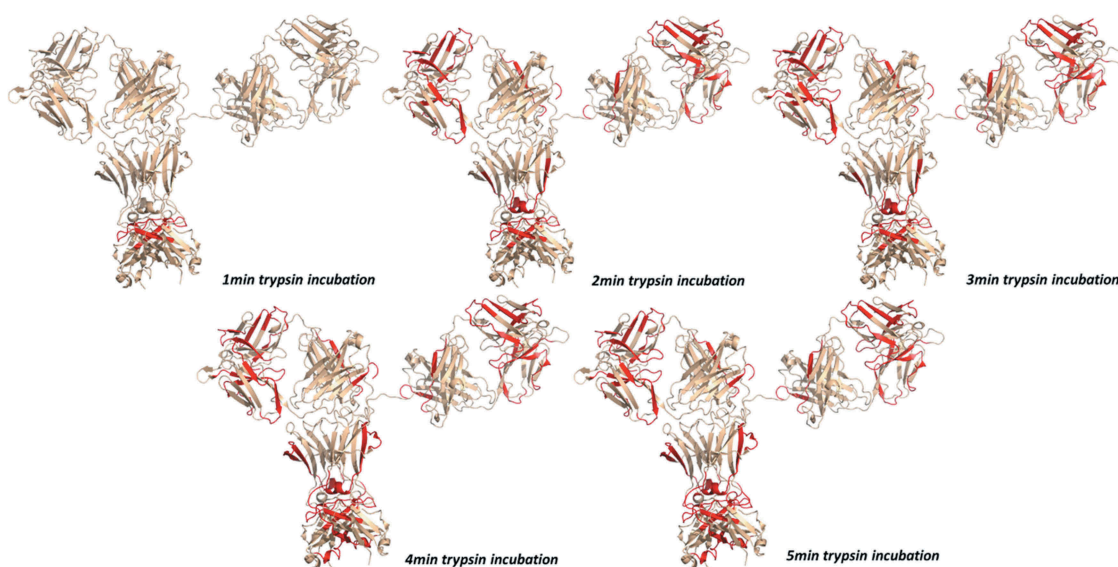


**Figure 1.** 3D IgG4 mAb structure – Trypsin digestion evolution – Cleaved peptides in red. The crystal structure of the mAb is the PDB 5DK3 with superposition of the Fab subunit crystal structure of the IgG4 mAb.<sup>34</sup>

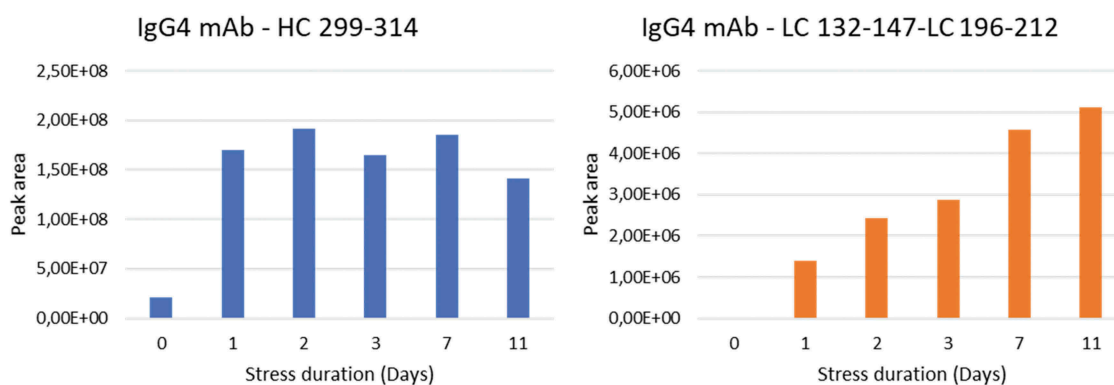


**Figure 2.** Histogram of two different peptides peak area in function of the temperature stress duration. The red line corresponds to the area threshold of the peptide to better assess a conformational change. Red line is missing for the crosslinked peptide LC 132–147–LC 196–212 because no peptide was detected at T0.

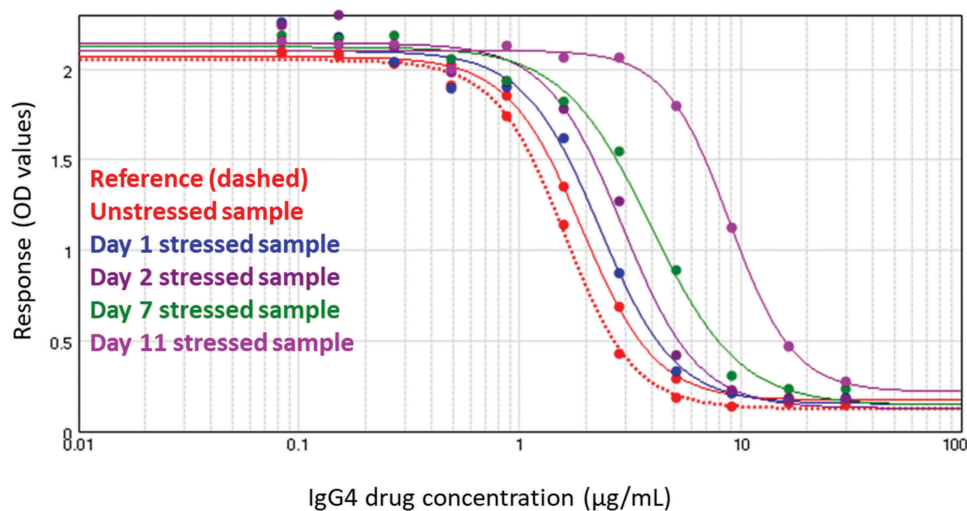


**Figure 3.** Dose-response curves generated in cell-based bioassay with a fixed concentration of the IgG4 drug target and serial dilutions of the drug. Samples come from heat degradation pathway study.

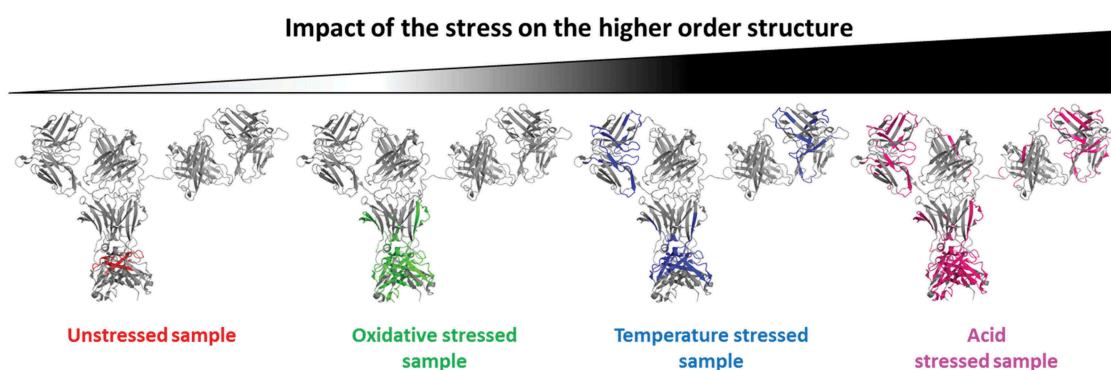


**Figure 4.** 3D IgG4 mAb structures with identified peptides after 5-min trypsin digestion in different colors depending on stress condition.

with trypsin before analysis with MALDI-HRMS. The quenching of the digestion was done at 1 min and just after the start of the digestion (less than 20 s of digestion) by adding 1% TFA solution.

Three different peptide groups can be differentiated based on the results shown in Table 2. The first group, comprising peptide HC 390–406, shown in white, was observed in the unstressed material after a 1-min trypsin incubation. This

peptide was also observed after the stress condition (heating at 50°C in a dry bath), but it was cleaved earlier in terms of trypsin incubation time (detected after several seconds at Days 1, 7, and 11). This is interpreted as indicating that the trypsin accessibility is increased by the stress, and, therefore, that the levels of unfolded or misfolded species increase during the stress.

**Table 2.** Summary table of the detected peptides after 1-min trypsin digestion by native peptide mapping from IgG4 samples exposed to temperature stress (50°C from Days 0 to 11). Green cell: peptide is detected; grey cell: peptide not detected. Peptides with asterisk mark (\*) were detected earlier in term of trypsin incubation time at Day 7 (except for LC 109–113 at Day 11).

Peptide	Day 0		Day 1		Day 7		Day 11	
	Trypsin digestion							
	<20s	1min	<20s	1min	<20s	1min	<20s	1min
HC 1-19								
HC 44-61								
HC 44-65								
HC 68-72*								
HC 77-87*								
HC 77-87 Ox								
HC 246-252*								
HC 286-298 G0F								
HC 299-314								
HC 320-331								
HC 324-331								
HC 336-357								
HC 336-341								
HC 338-357*								
HC 368-389								
HC 390-406								
HC 122-133-LC 213-219*								
HC 122-133-LC 217-219								
LC 1-18*								
LC 36-47								
LC 36-50								
LC 51-66*								
LC 52-66*								
LC 109-113*								
LC 113-131								
LC 114-131								
LC 155-188								

The second group of peptides, shown in orange in Table 2, was detected in the samples that were stressed for one day or more. Furthermore, as already observed for the first peptide group, peptides marked with asterisks were cleaved earlier (and detected after several seconds) at Day 7 and Day 11. Based on the two observations we made for this group, those peptides (in orange) are markers of the heat stress applied to the molecule. The third group of peptides, shown in yellow in Table 2, was detected in the samples that were stressed for at least seven days. These peptides represent a signature of more extensive heat stress of the molecule. The sequence of cleaved peptides released and the rate of release are indicative of the HOS and unfolding pathway of the mAb.

### Structure–activity relationships of stressed samples analysis

Temperature-stressed samples (50°C in a dry bath), for which HOS results were already reported in the previous section, were also analyzed by the CBA, and results are reported in Figure 3. The dose–response curves show a shift to the right as a function of the stress duration. This indicates that the stress condition negatively

impacting the biological activity of the drug correlates with the results of native peptide mapping (Figure 2 by routine UPLC-MS and Table 2 by MALDI-HRMS), which showed an evolution of the HOS with the duration of the heat stress.

Additional stress conditions were used to investigate the consequence of these conditions on the HOS of the mAb as measured by the native peptide mapping and the CBA. The following conditions were used: temperature (50°C for 14 days in oven), oxidative stress (0.1% H<sub>2</sub>O<sub>2</sub> for 14 days at 5°C) and acid stress (pH3 for 14 days at 5°C). Stressed materials were analyzed by native peptide mapping. These digests were then analyzed by MALDI-HRMS (in Table 3), by the routine UPLC-MS (Figure 5) and by CBA (Figure 6). The aim was to correlate the native peptide mapping results to the biological activity measured in bioassay as a function of the stressing agent.

As shown in Table 3, different peptides were observed depending on the stress conditions used. Oxidized and deamidated species were also observed in stressed samples by MALDI-HRMS. However, these modified peptide species were less abundant in the spectra compared to their corresponding native peptide. Based on the number of the cleaved



**Table 3.** Summary table of the IgG4 mAb identified peptides by MALDI-HRMS that were cleaved after 5-min trypsin incubation time for each stress condition and for the reference (unstressed material). In grey, absence of peptide; green, peptide observed. Peptides containing CDRs are in bold italic.

Peptide	Unstressed	Ox stress	Temp stress	Acid stress
HC 1-19				
HC 39-61				
<b><i>HC 44-61</i></b>				
<b><i>HC 44-65</i></b>				
HC 77-87				
HC 122-133-LC 217-219				
HC 246-252				
HC 286-298				
HC 299-314				
HC 299-317				
HC 342-357				
HC 358-367				
HC 368-389				
HC 390-406				
HC 414-436				
LC 1-18				
<b><i>LC 36-50</i></b>				
<b><i>LC 51-66</i></b>				
<b><i>LC 52-66</i></b>				

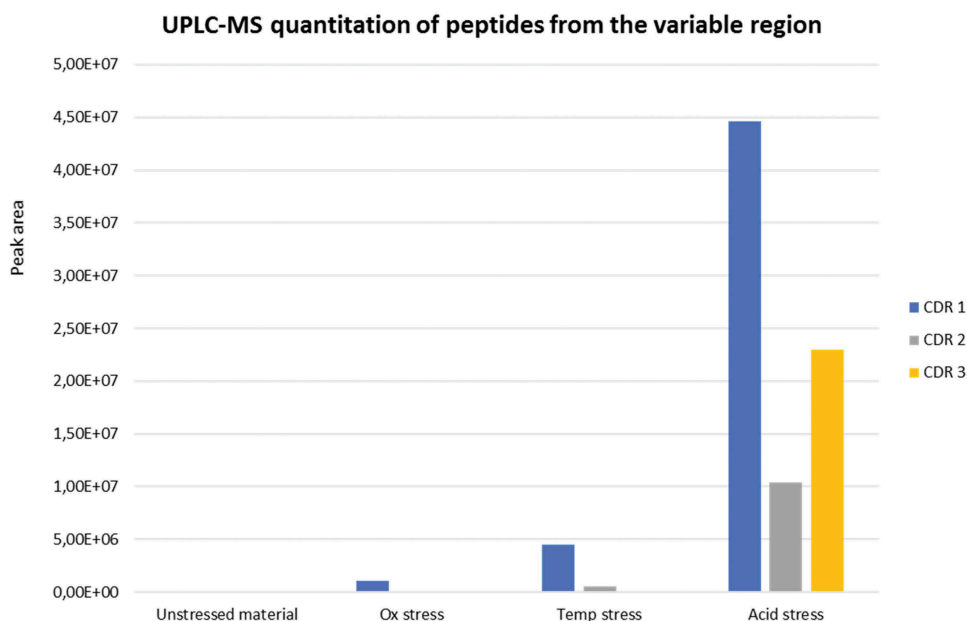


**Figure 5.** Peak area histogram of 3 CDR peptides peak area measured by UPLC-MS. CDR 1 area corresponds to the sum of the HC 44–61 and HC 44–65 peptide areas. CDR 2 area corresponds to the LC 36–50 peptide area. CDR 3 area corresponds to the sum of the LC 51–66 and LC 52–66 peptide areas.

peptides for each stress condition, the oxidative stress had less impact on the HOS structure of the mAb compared to the temperature stress and the acid stress, which was the most aggressive (Figure 4). This hypothesis was confirmed by

circular dichroism; results are shown in Figure 5 in the supplementary material.

Samples were then analyzed with the routine UPLC-MS system, and peptides from the CDRs (in bold italic in Table 3)

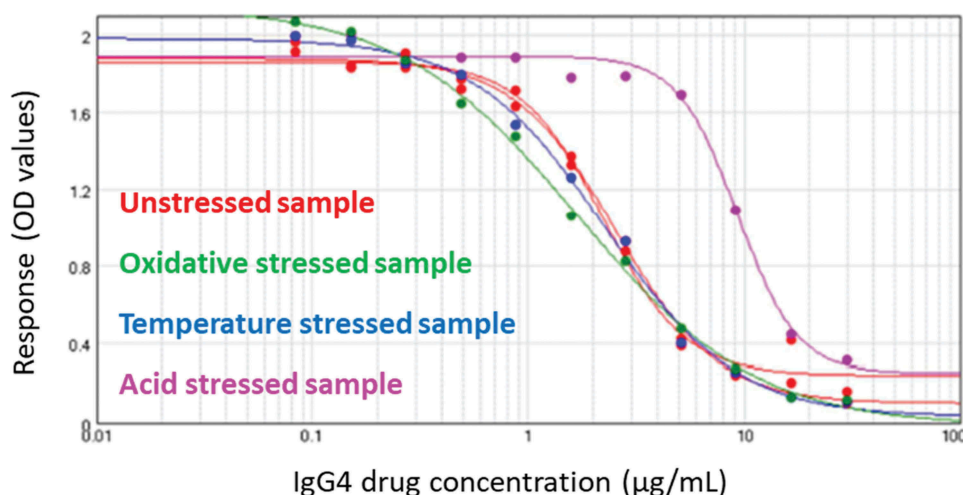


**Figure 6.** Dose-response curves generated in cell-based bioassay with a fixed concentration of the IgG4 drug target and serial dilutions of the drug. Samples come from different stress conditions.

were quantitated based on their peak area (see Figure 5). CDR peptides were chosen because of their role in the binding between the drug and its target. HC 77–87 peptide, which is included in the variable region close to a CDR of the mAb and only observed in acid-stressed sample results, was also quantitated (Figure 6 - SM6 in supplementary material). HC 77–87 peptide quantitation shows the same trend as the CDR peptides. HC 358–367, HC 414–436, and crosslinked HC 122–133-LC 217–219 peptides, which are located in the Fc subunit and the hinge region of the mAb, respectively, were not considered in the quantitation approach because of their location in the constant region of the mAb.

The areas of HC 44–61 and HC 44–65 have been summed, see Figure 5 and named “CDR 1” since both peptides were in this region of the molecule. The area of peptide LC 36–50 was reported as it contains another CDR and named “CDR 2”. The areas of LC 51–66 and LC 52–66 have also been summed and called “CDR3”. The acid-stressed sample presents higher levels of the CDR region containing peptides and of HC 77–87 peptide compared to the temperature-stressed sample and the oxidative-stressed sample (see Figure 6 in supplementary material). Moreover, no CDR peptide has been detected by the routine UPLC-MS system for the unstressed material (neither by MALDI-HRMS, see Table 3).

Comparison of the dose–response curves generated from the tested conditions (Figure 6) indicates that the acid-stressed sample (in purple) had a loss of biological activity (horizontal shift to the right) compared to the reference (in red). This observation could be explained by the fact that this stress was the most disruptive of the mAb’s HOS by native peptide mapping (Figure 5) and CD (see Figure 5 – SM5 in supplementary material). Furthermore, following the native peptide mapping results summarized in Table 3, four CDR peptides (in bold italic) were only identified in the acid-stressed sample.

Whilst additional-cleaved peptides compared to the reference were identified by native peptide mapping, no CDR peptides were detected by MALDI-HRMS and a negligible

amount of these peptides were measured by routine UPLC-MS. This observation demonstrates that only specific peptides are critical for the biological activity of the drug.

## Discussion

HOS determination is usually performed as part of characterization or comparability studies since the methods usually do not easily adapt to routine or QC settings due to the complexity of the methods, expense or availability of equipment and level of scientific expertise to interpret the results. For a HOS method to be easily adopted within a QC or routine testing environment, the assay method should be simple, fast, robust, not require specialized expertise or exotic equipment, and provide easily interpretable results regarding meeting defined specifications. Native peptide mapping fulfills many of the requirements to place HOS determination within a QC environment.

Limited proteolysis sample treatment, and especially the assumption that the protease accessibility in native-like conditions gives information about the HOS of the molecule, is increasingly accepted by the scientific community,<sup>33–35,38–44</sup> particularly to monitor the HOS of a mAb.<sup>32,36,45</sup> Table 1 and Figure 1 results suggest that the order of appearance of cleaved peptides is linked to: 1) the primary structure because of the specific cleavage sites of the trypsin, and 2) the HOS of the molecule due to the accessibility of the enzyme to cleavable sites present on the molecule. These assumptions are in line with previous publications<sup>32,36</sup> with an IgG4 mAb, but have never been demonstrated for an IgG1 subtype mAb with such a method (see Table 1 in supplementary material).

The stressed samples analysis and the comparison between stressed and reference samples (see Figure 2) highlight an important aspect: in addition to the order of appearance of cleaved peptides (determined in Table 1), the rate of appearance, and therefore the amount of these peptides at a given time, plays a key role in the comparison of the HOS state of the molecule. An increasing proportion of the molecules has an unfolded structure all along the stress period (reflected by the increasing number of cleaved peptides). As shown in Figure 2,

a comparison of each species using histograms could rapidly help the analyst to assess the conformation of the molecule during stability study, and such a comparison could reveal information on product stability and product knowledge in development. To introduce this method in QC, the choice of which cleaved peptides to follow is critical. For instance, the LC 132–147–LC 196–212 peptide (see Figure 2) is a good candidate because of its absence at Day 0 (unstressed material) and its presence on Day 1. Besides, the blue peptide HC 299–314 could be considered as a positive control of the trypsin digestion. In terms of specifications, it could be translated into the presence/absence of specific peptides to demonstrate the HOS of the molecule. In conclusion, limited-proteolysis-based method such as the native peptide mapping can be considered a stability-indicating method that is easily amenable in a QC routine laboratory. In this work, we confirmed the fitness-for-purpose of the native peptide mapping method by repeatability test, but also by applying such a method to another subtype of mAb never reported, IgG1 mAb.

As shown in Table 2, the native peptide mapping method gives rapid information on the unfolding pathway of the molecule for the stress condition (e.g., 50°C incubation in a dry bath). Different peptides detected by the method, especially the orange and yellow species could be representative of mAb regions that are sensitive to heat stress. Our interpretation of the results is that the overall molecule seems more flexible/open after the 50°C incubation. The root cause of the higher flexibility of the mAb could be explained by the disruption of non-covalent bonds or by the generation of modified residues (for example, oxidized or deamidated species) due to the stress, which could modify the tertiary structure of the protein,<sup>46</sup> or even by the combination of multiple phenomena. Further additional in-depth characterization of these stressed samples is needed to better identify what is the trigger of the unfolding. One example of such characterization could be similar to Patel *et al.* work who monitored, by multiple analytical techniques, the physicochemical stability of mAb mixtures to cover key structural attributes of the molecules. In conclusion, the authors stated that the formation of aggregation, a higher order structure attribute, was a trigger to the instability of the studied mAbs.<sup>47</sup> Other publications have mentioned that various degradation pathways (including the formation of aggregation but also the fragmentation from peptide bond cleavage) are triggered by a high-temperature stress.<sup>48–55</sup> In addition to having the ability to follow the unfolding pathway of a biotherapeutic, the method could be used to assess the biosimilarity of drugs in unstressed or under stress conditions. For instance, results from Pisupati *et al.* show similar levels of structural variation between biosimilar and innovator products by using different well-established HOS monitoring methods, such as size-exclusion chromatography, circular dichroism as well as bioassay.<sup>56</sup>

The relationship between the HOS determined by native peptide mapping and biological activity as measured by CBA was also evaluated. Two different stress studies were conducted to observe similarities with both techniques. The first stress campaign was the 50°C-heating condition in a dry bath to bridge the native peptide mapping data presented in the unfolding pathway study and CBA data. As presented, the structure of the mAb was evolving all along the stress period due to the identification of additional peptides at consecutive time points. As shown in Figure 3, a trend is also

observable for the dose-response curves indicating a progressive loss of biological activity of the drug all along the stress. This observation represents a new capacity of the native peptide mapping method to give information, not only on the HOS of the molecule as already stated in the previous sections and other publications, but also on its functionality/biological activity.

To continue the structure–activity relationship study, a second stress campaign was undertaken. The mAb was stressed with oxidation, high temperature, and acid stress conditions. These stressing conditions are similar to the commonly forced degradation conditions applied to mAbs,<sup>57</sup> and the purpose of the application of such conditions is to rapidly generate substantial levels of degradation in a short time period. Results shown in Table 3 and Figure 5 highlight that the HOS state located near the three CDR peptides of the acid-stressed sample is different compared to the other samples because of the trypsin accessibility difference. This difference is based on the CDR peptides detection by MALDI-HRMS (Table 3), but also by the quantitation by the routine UPLC-MS system (Figure 5). Indeed, in Figure 5, the acid stress has more effect on the HOS of the molecule's CDR compared to the temperature stress sample, even more than the oxidized-stressed sample because it was possible for the trypsin to cleave more of the molecule during the same digestion duration. On the other hand, results shown in Figure 6 indicate a drop in the biological activity only for this acid-stressed sample, demonstrating the relation between both techniques/properties of the drug. Hence, the major breakthrough of this work relies on the structure–activity relationship, which has been highlighted by comparing bioassay and native peptide mapping results with unstressed and multiple stressed materials. The reported results show the impact of various stresses on the HOS (confirmed by CD results) and on the mechanism of action of the drug measured by CBA. This novel capacity of limited proteolysis-based methods opens up new opportunities for the biopharmaceutical analytical community to assess the biological activity of biotherapeutics more rapidly than with the current bioassay-based methods such as ELISA and CBA.

In conclusion, given that the new relationship between the structure and the activity of the mAb, native peptide mapping could be considered a novel multi-attribute method in stability and in batch comparability studies<sup>58</sup> to assess: 1) the integrity of the mAb with respect to its HOS and 2) the activity of the product by monitoring more precisely the HOS of the CDR regions.

## Materials and methods

Both full-length humanized IgG4 and IgG1 mAbs was manufactured in-house by UCB and were used for this study from available batches. IgG4-mAb formulation buffer is composed of 30 mM L-Histidine, 250mM L-Proline, 0.03% (w/v) Polysorbate 80, pH 5.6. IgG1 mAb formulation buffer is composed of 55 mM sodium acetate, 220 mM Glycine, 0.04% (w/v) Polysorbate 80, pH 5.0.



## Generation of stressed samples

### Heat

The IgG4-mAb was incubated at 50°C in a dry bath during the stress. 100 µL was sampled at each time point (Day 0, Day 1, Day 2, Day 7, Day 11) and stored at ≤−60°C until analysis.

### Acid – pH 3

The IgG4-mAb was buffer exchanged into 100 mM sodium citrate (Merck, 1613859) buffer at pH 3.0 and incubated at 2–8°C for 14 days. At the end of the incubation, sample was buffer exchanged back into formulation buffer.

### Oxidation

H<sub>2</sub>O<sub>2</sub> (Merck, 16911) was added to a 500 µL aliquot of IgG4-mAb to a final concentration of 0.1% (w/w) and incubated at 2–8°C for 14 days. At the end of the stress, sample is buffer exchanged back into formulation buffer.

### Temperature

The IgG4-mAb is incubated at 50°C in an oven for 14 days and stored at ≤−60 °C until analysis.

## Native peptide mapping analysis by matrix-assisted laser desorption ionization mass spectrometry

All samples were subjected to protease digestion by addition of trypsin (Promega, V5117) in Hank's Balanced Salt Solution (Merck, H6648) at 37°C. The ratio of protein to enzyme was 10:1 (w:w); the protein concentration during digestion was 2 mg/mL. The digestion was stopped by the addition of TFA (Merck, 1.08262) to a final concentration of 0.8% v/v after the required time for the digestion step had elapsed. For the time zero samples, the addition of the enzyme was immediately followed by the addition of the TFA. MALDI-MS experiments were performed using UltrafleXtreme mass spectrometer (Bruker Daltonics) with a mass range from 500 to 7000 m/z. The matrix solution was α-Cyano-4-hydroxycinnamic acid (Bruker Daltonics, 8255344) 1.4 mg/mL solubilized in 85/15 acetonitrile (Biosolve, 01207801)/H<sub>2</sub>O (milliQ) TFA 0.1% (Merck, 1.08262), 10 mM NH<sub>4</sub>H<sub>2</sub>PO<sub>4</sub> (Merck, 216003).

## Circular dichroism

Spectra were recorded using a Chirascan Plus spectrometer (Aimil). Data were collected at a scan rate of 0.5 nm s<sup>−1</sup> over the range 250 nm to 320 nm for near UV CD using a cell pathlength of 10 mm. Far-UV data were collected at a scan rate of 0.5 nm s<sup>−1</sup> over the range 200 nm to 260 nm for far UV CD using a cell pathlength of 0.2 mm.

All spectra were corrected for buffer contribution and concentration corrected ( $A_{280}$  reading) and the CD values (mdeg) converted to mean residue molar ellipticity (deg cm<sup>2</sup>dmol<sup>−1</sup>residue<sup>−1</sup>). Measurements were taken at 0.75 mg/mL mAb concentration for both near and far-UV CD.

## Native peptide mapping analysis by routine UPLC-MS

Reversed phase-Ultra Performance Liquid Chromatography (RP-UPLC) was performed using Waters H-Class Acquity chromatography system coupled to quadrupole mass spectrometer QDa from Waters using electrospray ionization (ESI).

10 µL (10 µg of protein) of the digested sample was injected on a CSH C<sub>18</sub> 1.7 µm 2.1 mm × 150 mm column (Waters) with the column oven maintained at 40°C. The mobile phase had a flow rate of 0.4 mL/min. The chromatography was performed using milliQ water containing 0.1% formic acid (Merck, 1.00264) for mobile phase A and acetonitrile (Biosolve, 01207801) containing 0.1% formic acid (Merck, 1.00264) for mobile phase B. Gradient was applied as follows: B was increased from 3% to 18% over 19 min, from 18% to 30% over 25 min and from 30% to 37% over 3 min, equilibration time 1 min.

The QDa quadrupole was operated in positive ion mode with a capillary voltage of 1.5 kV and a sample cone voltage of 10 V. Acquisitions were performed over the range 300–1250 m/z. Single ion recording mode was used for each peptide identified from Native peptide mapping analysis by MALDI-MS. Data analysis was performed with Empower 3.0 from Waters.

## Cell-based bioassay

The cell-based bioassay used to measure the relative potency of the mAb was designed to be representative of its mechanism of action (IgG recycling). The assay is composed of two testing phases. The first step consisted of the incubation of a responsive cell line (MDCK cells (ATCC CCL-34™) over-expressing human drug target) with serial dilutions of the mAb and a fixed concentration of biotinylated human IgG. Binding of the mAb to its target impairs IgG recycling that is further evaluated in ELISA.

The second assay step consists of the quantification of a non-degraded biotinylated human IgG by ELISA. Based on the IgG recycling assay principle, the mAb potency is evaluated for its ability to inhibit the recycling of a biotinylated-IgG solution. Consequently, there is an inverse relationship between the mAb concentration and the amount of biotinylated IgGs measured in ELISA. Relative potency is calculated as the EC<sub>50</sub> ratio between standard and test sample dose-response curve preparations, in agreement with the corresponding European/US Pharmacopoeia chapters.<sup>59,60</sup>

## Acknowledgments

We would like to acknowledge Sandrine Van Leugenhaeghe and Gauthier Husson for performing some of the repeatability assessment work and Maria Zaccarini for undertaking the circular dichroism experiments.

## Disclosure of Potential Conflicts of Interest

No potential conflicts of interest were disclosed.

## ORCID

Michel Degueldre  <http://orcid.org/0000-0002-6034-0539>Gaël Debauxe  <http://orcid.org/0000-0002-6720-7423>

## References

1. ICH Q8. Pharmaceutical development. [https://www.ich.org/fileadmin/Public\\_Web\\_Site/ICH\\_Products/Guidelines/Quality/Q8\\_R1/Step4/Q8\\_R2\\_Guideline.pdf](https://www.ich.org/fileadmin/Public_Web_Site/ICH_Products/Guidelines/Quality/Q8_R1/Step4/Q8_R2_Guideline.pdf), 21 January 2019.
2. ICH Q6B. Specifications: test procedures and acceptance criteria for biotechnological/biological products. [https://www.ich.org/fileadmin/Public\\_Web\\_Site/ICH\\_Products/Guidelines/Quality/Q6B/Step4/Q6B\\_Guideline.pdf](https://www.ich.org/fileadmin/Public_Web_Site/ICH_Products/Guidelines/Quality/Q6B/Step4/Q6B_Guideline.pdf), 21 January 2019
3. ICH Q7. Good manufacturing practice guide for active pharmaceutical ingredients. [https://www.ich.org/fileadmin/Public\\_Web\\_Site/ICH\\_Products/Guidelines/Quality/Q7/Step4/Q7\\_Guideline.pdf](https://www.ich.org/fileadmin/Public_Web_Site/ICH_Products/Guidelines/Quality/Q7/Step4/Q7_Guideline.pdf), 21 January 2019.
4. Alt N, Zhang TY, Motchnik P, Taticek R, Quarmby V, Schlothauer T, Beck H, Emrich T, Harris RJ. Determination of critical quality attributes for monoclonal antibodies using quality by design principles. *Biologicals*. 2016;44(5):291–305. doi:10.1016/j.biologicals.2016.06.005.
5. Swain S, Padhy R, Jena BR, Babu SM. Quality by design: concept to applications. *Curr Drug Discov Technol*. 2018. doi:10.2174/1570163815666180308142016.
6. Kepert JF, Cromwell M, Engler N, Finkler C, Gellermann G, Gennaro L, Harris R, Iverson R, Kelley B, Krummen L, et al. Establishing a control system using QbD principles. *Biologicals*. 2016;44(5):319–31. doi:10.1016/j.biologicals.2016.06.003.
7. Rosario M, Dirks NL, Milch C, Parikh A, Bargfrede M, Wyant T, Fedyk E, Fox I. A review of the clinical pharmacokinetics, pharmacodynamics, and immunogenicity of vedolizumab. *Clin Pharmacokinet*. 2017;56(11):1287–301. doi:10.1007/s40262-017-0546-0.
8. Bhunia D, Chowdhury R, Bhattacharyya K, Ghosh S. Fluorescence fluctuation of an antigen-antibody complex: circular dichroism, FCS and smFRET of enhanced GFP and its antibody. *Phys Chem Chem Phys*. 2015;17(38):25250–59. doi:10.1039/c5cp04908c.
9. Lin JC, Glover ZK, Sreedhara A. Assessing the utility of circular dichroism and FTIR spectroscopy in monoclonal-antibody comparability studies. *J Pharm Sci*. 2015;104(12):4459–66. doi:10.1002/jps.24683.
10. Kats M, Richberg PC, Hughes DE. Conformational diversity and conformational transitions of a monoclonal antibody monitored by circular dichroism and capillary electrophoresis. *Anal Chem*. 1995;67:2943–48.
11. Joshi V, Shivach T, Yadav N, Rathore AS. Circular dichroism spectroscopy as a tool for monitoring aggregation in monoclonal antibody therapeutics. *Anal Chem*. 2014;86(23):11606–13. doi:10.1021/ac503140j.
12. Ellett LJ, Johanssen VA. Analysis of prion protein conformation using circular dichroism spectroscopy. *Methods Mol Biol*. 2017;1658:27–34. doi:10.1007/978-1-4939-7244-9\_3.
13. Nagarkar RP, Murphy BM, Yu X, Manning MC, Al-Azzam WA. Characterization of protein higher order structure using vibrational circular dichroism spectroscopy. *Curr Pharm Biotechnol*. 2013;14:199–208.
14. Toride King M, Brooks CL. Epitope mapping of antibody-antigen interactions with X-Ray crystallography. *Methods Mol Biol*. 2018;1785:13–27. doi:10.1007/978-1-4939-7841-0\_2.
15. Loyau J, Didelot G, Malinge P, Ravn U, Magistrelli G, Depoisier JF, Pontini G, Poitevin Y, Kosco-Vilbois M, Fischer N, et al. Robust antibody-antigen complexes prediction generated by combining sequence analyses, mutagenesis, in vitro evolution, X-ray crystallography and in silico docking. *J Mol Biol*. 2015;427(16):2647–62. doi:10.1016/j.jmb.2015.05.016.
16. Inouye H, Houde D, Temel DB, Makowski L. Utility of solution X-Ray scattering for the development of antibody biopharmaceuticals. *J Pharm Sci*. 2016;105(11):3278–89. doi:10.1016/j.xphs.2016.07.021.
17. Ghasriani H, Hodgson DJ, Brinson RG, McEwen I, Buhse LF, Kozlowski S, Marino JP, Aubin Y, Keire DA. Precision and robustness of 2D-NMR for structure assessment of filgrastim biosimilars. *Nat Biotechnol*. 2016;34(2):139–41. doi:10.1038/nbt.3474.
18. Chen K, Long DS, Lute SC, Levy MJ, Brorson KA, Keire DA. Simple NMR methods for evaluating higher order structures of monoclonal antibody therapeutics with quinary structure. *J Pharm Biomed Anal*. 2016;128:398–407. doi:10.1016/j.jpba.2016.06.007.
19. Brinson RG, Ghasriani H, Hodgson DJ, Adams KM, McEwen I, Freedberg DI, Chen K, Keire DA, Aubin Y, Marino JP. Application of 2D-NMR with room temperature NMR probes for the assessment of the higher order structure of filgrastim. *J Pharm Biomed Anal*. 2017;141:229–33. doi:10.1016/j.jpba.2017.03.063.
20. Litwinczuk A, Ryu SR, Nafie LA, Lee JW, Kim HI, Jung YM, Czarnik-Matuszewicz BÉ. The transition from the native to the acid-state characterized by multi-spectroscopy approach: study for the holo-form of bovine + $\beta$ -lactalbumin. *Biochimica Et Biophysica Acta*. 2014;1844(3):593–606. doi:10.1016/j.bbapap.2013.12.018.
21. Arbogast LW, Brinson RG, Marino JP. Application of natural isotopic abundance  $^1\text{H}^{13}\text{C}$ - and  $^1\text{H}^{15}\text{N}$ -correlated two-dimensional NMR for evaluation of the structure of protein therapeutics. In: Abelson J, Simon M, Verdine G, Pyle A, editors. *Methods in enzymology isotope labeling of biomolecules - applications*. 2016; Vol. 566. 3–34.
22. Ferguson CN, Gucinski-Ruth AC. Evaluation of ion mobility-mass spectrometry for comparative analysis of monoclonal antibodies. *J Am Soc Mass Spectrom*. 2016;27(5):822–33. doi:10.1007/s13361-016-1369-1.
23. Nesmelov YE, Thomas DD. Protein structural dynamics revealed by site-directed spin labeling and multifrequency EPR. *Biophys Rev*. 2010;2(2):91–99. doi:10.1007/s12551-010-0032-5.
24. Rathore AS, Winkle H. Quality by design for biopharmaceuticals. *Nat Biotech*. 2009;27(1):26–34. doi:10.1038/nbt0109-26.
25. Luciani F, Galluzzo S, Gaggioli A, Kruse NA, Venneugues P, Schneider CK, Pini C, Melchiorri D. Implementing quality by design for biotech products: are regulators on track? *MABs*. 2015;7(3):451–55. doi:10.1080/19420862.2015.1023058.
26. Xu Y, Wang D, Mason B, Rossomando T, Li N, Liu D, Cheung JK, Xu W, Raghava S, Katiyar A, et al. Structure, heterogeneity and developability assessment of therapeutic antibodies. *MABs*. 2019;11(2):239–64. doi:10.1080/19420862.2018.1553476.
27. Rogstad S, Faustino A, Ruth A, Keire D, Boyne M, Park J. A retrospective evaluation of the use of mass spectrometry in FDA biologics license applications. *J Am Soc Mass Spectrom*. 2017;28(5):786–94. doi:10.1007/s13361-016-1531-9.
28. Rathore D, Faustino A, Schiel J, Pang E, Boyne M, Rogstad S. The role of mass spectrometry in the characterization of biologic protein products. *Expert Rev Proteomics*. 2018;15(5):431–49. doi:10.1080/14789450.2018.1469982.
29. Yan Y, Wei H, Fu Y, Jusuf S, Zeng M, Ludwig R, Krystek SR, Chen G, Tao L, Das TK. Isomerization and oxidation in the complementarity-determining regions of a monoclonal antibody: a study of the modification-structure-function correlations by hydrogen-deuterium exchange mass spectrometry. *Anal Chem Am Chem Soc*. 2016;88:2041–50. doi:10.1021/acs.analchem.5b02800.
30. Gau BC, Sharp JS, Rempel DL, Gross ML. Fast photochemical oxidation of protein footprints faster than protein unfolding. *Anal Chem*. 2009;81(16):6563–71. doi:10.1021/ac901054w.
31. Rattan AK. Data integrity: history, issues, and remediation of issues. *PDA J Pharm Sci Technol*. 2018;72(2):105–16. doi:10.5731/pdajpst.2017.007765.
32. Perrin C, Burkitt W, Perraud X, O'Hara J, Jone C. Limited proteolysis and peptide mapping for comparability of

- biopharmaceuticals: an evaluation of repeatability, intra-assay precision and capability to detect structural change. *J Pharm Biomed Anal.* 2016;123:162–72. doi:10.1016/j.jpba.2016.02.005.
33. Fontana A, de Laureto PP, Spolaore B, Frare E, Picotti P, Zambonin M. Probing protein structure by limited proteolysis. *Acta Biochim Pol.* 2004;51(2):299–321.
  34. Spolaore B, Bermejo R, Zambonin M, Fontana A. Protein interactions leading to conformational changes monitored by limited proteolysis: apo form and fragments of horse cytochrome c. *Biochemistry.* 2001;40(32):9460–68. doi:10.1021/bi010582c.
  35. Fontana A, de Laureto PP, De Filippis V, Scaramella E, Zambonin M. Probing the partly folded states of proteins by limited proteolysis. *Fold Des.* 1997;2(2):R17–R26. doi:10.1016/S1359-0278(97)00010-2.
  36. Cao X, Flagg SC, Li X, Chennamsetty N, Balakrishnan G, Das TK. Quadrupole dalton-based controlled proteolysis method for characterization of higher order protein structure. *Anal Chem.* 2019;91(8):5339–45. doi:10.1021/acs.analchem.9b00306.
  37. Xu W, Jimenez RB, Mowery R, Luo H, Cao M, Agarwal N, Ramos I, Wang X, Wang J. A quadrupole dalton-based multi-attribute method for product characterization, process development, and quality control of therapeutic proteins. *MAbs.* 2017;9(7):1186–96. doi:10.1080/19420862.2017.1364326.
  38. Piazza I, Kochanowski K, Cappelletti V, Fuhrer T, Noor E, Sauer U, Picotti P. A map of protein-metabolite interactions reveals principles of chemical communication. *Cell.* 2018;172(1–2):358–372 e23. doi:10.1016/j.cell.2017.12.006.
  39. Schopper S, Kahraman A, Leuenberger P, Feng Y, Piazza I, Muller O, Boersema PJ, Picotti P. Measuring protein structural changes on a proteome-wide scale using limited proteolysis-coupled mass spectrometry. *Nat Protoc.* 2017;12(11):2391–410. doi:10.1038/nprot.2017.100.
  40. Feng Y, De Franceschi G, Kahraman A, Soste M, Melnik A, Boersema PJ, de Laureto PP, Nikolaev Y, Oliveira AP, Picotti P. Global analysis of protein structural changes in complex proteomes. *Nat Biotechnol.* 2014;32(10):1036–44. doi:10.1038/nbt.2999.
  41. Picotti P, Dewilde S, Fago A, Hundahl C, De Filippis V, Moens L, Fontana A. Unusual stability of human neuroglobin at low pH—molecular mechanisms and biological significance. *Febs J.* 2009;276(23):7027–39. doi:10.1111/j.1742-4658.2009.07416.x.
  42. Codutti L, Picotti P, Marin O, Dewilde S, Fogolari F, Corazza A, Viglino P, Moens L, Esposito G, Fontana A. Conformational stability of neuroglobin helix F—possible effects on the folding pathway within the globin family. *Febs J.* 2009;276(18):5177–90. doi:10.1111/j.1742-4658.2009.07214.x.
  43. Bisetto E, Picotti P, Giorgio V, Alverdi V, Mavelli I, Lippe G. Functional and stoichiometric analysis of subunit e in bovine heart mitochondrial F(0)F(1)ATP synthase. *J Bioenerg Biomembr.* 2008;40(4):257–67. doi:10.1007/s10863-008-9183-5.
  44. Park C, Marqusee S. Pulse proteolysis: a simple method for quantitative determination of protein stability and ligand binding. *Nat Methods.* 2005;2(3):207–12. doi:10.1038/nmeth740.
  45. Goswami D, Zhang J, Bondarenko PV, Zhang Z. MS-based conformation analysis of recombinant proteins in design, optimization and development of biopharmaceuticals. *Methods.* 2018;144:134–51. doi:10.1016/j.ymeth.2018.04.011.
  46. Shah DD, Singh SM, Mallela KMG. Effect of chemical oxidation on the higher order structure, stability, aggregation, and biological function of interferon alpha-2a: role of local structural changes detected by 2D NMR. *Pharm Res.* 2018;35(12):232. doi:10.1007/s11095-018-2518-y.
  47. Patel A, Gupta V, Hickey J, Nightlinger NS, Rogers RS, Siska C, Joshi SB, Seaman MS, Volkin DB, Kerwin BA. Coformulation of broadly neutralizing antibodies 3BNC117 and PGT121: analytical challenges during preformulation characterization and storage stability studies. *J Pharm Sci.* 2018;107(12):3032–46. doi:10.1016/j.xphs.2018.08.012.
  48. Xiang T, Lundell E, Sun Z, Liu H. Structural effect of a recombinant monoclonal antibody on hinge region peptide bond hydrolysis. *J Chromatogr B Analyt Technol Biomed Life Sci.* 2007;858(1–2):254–62. doi:10.1016/j.jchromb.2007.08.043.
  49. Liu H, Gaza-Bulsecu G, Lundell E. Assessment of antibody fragmentation by reversed-phase liquid chromatography and mass spectrometry. *J Chromatogr B Analyt Technol Biomed Life Sci.* 2008;876(1):13–23. doi:10.1016/j.jchromb.2008.10.015.
  50. Zhang A, Singh SK, Shirts MR, Kumar S, Fernandez EJ. Distinct aggregation mechanisms of monoclonal antibody under thermal and freeze-thaw stresses revealed by hydrogen exchange. *Pharm Res.* 2012;29(1):236–50. doi:10.1007/s11095-011-0538-y.
  51. Luo Q, Joubert MK, Stevenson R, Ketchem RR, Narhi LO, Wypych J. Chemical modifications in therapeutic protein aggregates generated under different stress conditions. *J Biol Chem.* 2011;286(28):25134–44. doi:10.1074/jbc.M110.160440.
  52. Liu H, Gaza-Bulsecu G, Sun J. Characterization of the stability of a fully human monoclonal IgG after prolonged incubation at elevated temperature. *J Chromatogr B Analyt Technol Biomed Life Sci.* 2006;837(1–2):35–43. doi:10.1016/j.jchromb.2006.03.053.
  53. Hawe A, Kasper JC, Friess W, Jiskoot W. Structural properties of monoclonal antibody aggregates induced by freeze-thawing and thermal stress. *Eur J Pharm Sci.* 2009;38(2):79–87. doi:10.1016/j.ejps.2009.06.001.
  54. Fesinmeyer RM, Hogan S, Saluja A, Brych SR, Kras E, Narhi LO, Brems DN, Gokarn YR. Effect of ions on agitation- and temperature-induced aggregation reactions of antibodies. *Pharm Res.* 2009;26(4):903–13. doi:10.1007/s11095-008-9792-z.
  55. Alexander AJ, Hughes DE. Monitoring of IgG antibody thermal stability by micellar electrokinetic capillary chromatography and matrix-assisted laser desorption/ionization mass spectrometry. *Anal Chem.* 1995;67:3626–32.
  56. Pisupati K, Benet A, Tian Y, Okbazghi S, Kang J, Ford M, Saveliev S, Sen KI, Carlson E, Tolbert TJ, et al. Biosimilarity under stress: A forced degradation study of remicade(R) and remsima. *MAbs.* 2017;9(7):1197–209. doi:10.1080/19420862.2017.1347741.
  57. Nowak CK, Cheung JM, Dellatore S, Katiyar A, Bhat R, Sun J, Ponniah G, Neill A, Mason B, Beck A, et al. Forced degradation of recombinant monoclonal antibodies: A practical guide. *MAbs.* 2017;9(8):1217–30. doi:10.1080/19420862.2017.1368602.
  58. Ambrogelly A, Gozo S, Katiyar A, Dellatore S, Kune Y, Bhat R, Sun J, Li N, Wang D, Nowak C, et al. Analytical comparability study of recombinant monoclonal antibody therapeutics. *MAbs.* 2018;10(4):513–38. doi:10.1080/19420862.2018.1438797.
  59. EP. Chapter 5.3: Statistical analysis of Results of Biological Assays and Tests. *Eur Pharmacopoeia.* 2016;9(2):4353–4381.
  60. USP. Chapter 1034: Analysis of Biological Assays. *U S Pharmacopeial Convention.* 2018;5:6818